32ND INTERNATIONAL COSMIC RAY CONFERENCE, BEIJING 2011

Measurement of the CR light component primary spectrum

B. PANICO[1,2], G. DI SCIASCIO[1] AND S. CATALANOTTI[3] FOR THE ARGO-YBJ COLLABORATION
[1]*INFN, Sezione Roma Tor Vergata, Via della Ricerca Scientifica 1, Roma, Italy*
[2] *Dipartimento di Fisica, Universitá Roma "Tor Vergata", via della Ricerca Scientifica 1, Roma, Italy*
[3] *Dipartimento di Fisica, Università "Federico II" and INFN sez. Napoli, Napoli, Italy*
beatrice.panico@roma2.infn.it,disciascio@roma2.infn.it, catalanotti@na.infn.it

Abstract: The ARGO-YBJ experiment, located at the Yangbajing Cosmic Ray Laboratory (Tibet, 4300 m a.s.l., 606 g/cm^2) has an high segmentation that allows the detection of air showers with greater detail and lower energy threshold (a few hundred GeV) compared to other EAS arrays. The spectrum of the primary Cosmic Ray light (p+He) component in the energy range $\sim$10 - 100 TeV is measured selecting quasi-vertical showers with the reconstructed core position located in a 40$\times$40 m^2 fiducial area. The results are compared with other measurements carried out with direct methods.

Keywords: Extensive Air showers, Cosmic Ray Spectrum, ARGO-YBJ

1 Introduction

There is a general consensus that Cosmic Rays (CRs) up to the "knee" ($\sim 3 \cdot 10^{15}$ eV) originate in Galactic Supernova Remnants accelerated by the first order Fermi mechanism in shock waves. The theoretical modelling of this mechanism can reproduce the measured spectra and composition of CRs. The bulk of primary CRs at the energies well below the knee are proton and helium nuclei. Recent measurements carried out by the balloon-borne CREAM experiment [1, 2] show that the proton and helium spectra from 2.5 to 250 TeV are both flatter compared to the lower energy measurements. In particular, the proton spectrum in this energy range is found harder than the value quoted in [3] and obtained by fitting many previous direct measurements. In addition, the proton and helium fluxes measured by CREAM are consistent with the measurements of JACEE [4] and higher, particularly for helium, with respect to RUNJOB [5]. The evolution of the proton and helium spectra and their subtle differences can be an indication of the contribution of different populations of CR sources operating in environments with different chemical compositions [6].

In the knee region the measurements of the CR primary spectrum are carried out only by EAS arrays and the current experimental results are still conflicting. In the standard picture the mass of the knee is light [7, 8] being due to the steepening of the p and He spectra. However, increasing the altitude of the experiment locations the average mass of the knee increases as well. In fact, the results of the Tibet ASγ and the BASJE experiments, located at 4300 m a.s.l and at 5200 m a.s.l. respectively, favour a heavier composition because the proton component is no more dominant at the knee [9, 10].

Therefore, protons are the key component for understanding the origin of the knee. In addition, precise knowledge of their fluxes may allow one to calculate the yield of rare secondary CRs as antiprotons and positrons and establish the expected fluxes of the atmospheric neutrinos. Data in the TeV range are important for the neutrino-induced upward muon calculations.

Additional information on the proton spectrum has been obtained from the high energy branch of the sea level muon spectrum [11] and from the energy spectrum of the hadronic component in EAS[12]. A measurement of the Cherenkov light yield at different core distances in EAS performed by the EAS-TOP and MACRO experiments has been used to infer the helium flux at 80 TeV, resulting twice larger than that obtained by JACEE [7].

The ARGO-YBJ detector is well suited to study the spectrum of the "light component" at energies $<$100 TeV by exploiting its digital readout. In addition, by exploiting the analog readout, the experiment is able to extend its energetic range up to the knee. The capability to measure the CR spectrum over more than 3 energy decades (TeV-PeV) makes ARGO-YBJ the only experiment suitable to anchor ground-based data to direct measurements.

In this paper we report on the measurement of the spectrum of the primary CR light (p+He) component in the energy range $\sim$10 - 100 TeV selecting quasi-vertical showers (zenith angle $\theta < 15^\circ$) with the reconstructed core position located in a 40$\times$40 m^2 fiducial area. The results are compared with measurements carried out with direct methods.

2 The ARGO-YBJ experiment

The detector is composed of a central carpet large $\sim$74$\times$ 78 m^2, made of a single layer of Resistive Plate Chambers (RPCs) with $\sim$93$\%$ of active area, enclosed by a guard ring partially ($\sim$20$\%$) instrumented up to $\sim$100$\times$110 m^2. The apparatus has a modular structure, the basic data acquisition element being a cluster (5.7$\times$7.6 m^2), made of 12 RPCs (2.8$\times$1.25 m^2 each). Each chamber is read by 80 external strips of dimension 6.75$\times$61.8 cm^2 (the spatial pixels), logically organized in 10 independent pads of area 55.6$\times$61.8 cm^2 which represent the time pixels of the detector. The readout of 18360 pads and 146880 strips is the experimental output of the detector [13]. The relation between strip and pad multiplicities has been measured and found in fine agreement with the Monte Carlo prediction [13]. In addition, in order to extend the dynamical range up to PeV energies, each chamber is equipped with two large size pads (139$\times$123 cm^2) to collect the total charge developed by the particles hitting the detector [14]. The central carpet contains 130 clusters (hereafter, ARGO-130) and the full detector is composed of 153 clusters for a total active surface of $\sim$6700 m^2. Due to the small pixel size, the detector is able to record events with a particle density exceeding 0.003 particles m^{-2}, keeping good linearity up to a core density of about 15 particles m^{-2}. This high granularity allows a complete and detailed three-dimensional reconstruction of the front of air showers with an energy threshold of a few hundred GeV. Showers induced by high energy primaries ($>$ 100 TeV) are also imaged by the analog read-out of the large size pads [14].

The whole system, in smooth data taking since July 2006 firstly with ARGO-130, is in stable data taking with the full apparatus of 153 clusters since November 2007 with the trigger condition N$_{trig}$ = 20 pads and a duty cycle $\geq$86%. The trigger rate is 3.5 kHz with a dead time of 4$\%$.

3 Data analysis

The reconstruction of the shower parameters is split into the following steps. First, the shower core position is derived with the Maximum Likelihood method from the lateral density distribution of the secondary particles [15]. In the second step, given the core position, the shower axis is reconstructed by means of an iterative unweighted planar fit able to reject the time values belonging to the non-gaussian tails of the arrival time distributions. Finally, a conical correction with a slope fixed to α = 0.03 ns/m is applied to the surviving hits in order to improve the angular resolution [16].

The analysis reported in this paper refers to events collected in 2009 after the following selections: (1) more than 251 strips on the ARGO-130 carpet; (2) zenith angle of the shower arrival direction less than 15°; (3) reconstructed core position inside area A$_{fid}$=40$\times$40 m^2 centered on the detector. This selection provides that the contamination

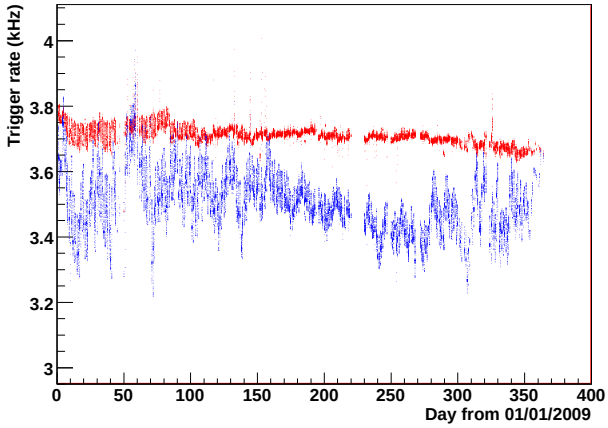

Figure 1: Event rates before (blue points) and after (red points) the correction of barometric and bad pad effects (see text for details).

of external events erroneously reconstructed inside A$_{fid}$ is less than 15% and the reconstruction efficiency $>$85$\%$.

In addition, a sample of high quality runs has been selected by requiring that the total number of pads dead or with a counting rate less than 50$\%$ of the mean value (”bad” pads) is less than 3$\%$. In such a way only runs with less than about 500 bad pads (over 15600) have been used in the analysis. We also excluded from the analysis all data with a pressure value larger than 3 standard deviations from the mean value. This leads to a data set of about 250 days.

The measured event rate is modulated on a long time period by the fluctuations of the shower development and instrumental response. In order to correct these effects, the correlation with atmospheric pressure and temperature has been investigated. We found, as expected, the barometric effect dominant. In Fig.1, for example, the rate of all the events starting from the trigger threshold N$_{trig}$ = 20, without any core selection, is shown by blue points. The horizontal axis represents the time elapsed from January 1, 2009 counted in bins of 1 day. The rates are normalized at a definite number of efficient pads and at the nominal pressure at YBJ site, following the relation

$$R = R_0\,[1-\alpha(N-N_0)]\,e^{-\beta(p-p_0)} \qquad (1)$$

where R$_0$ is the daily measured rate, N is the number of bad pads whose mean number is N$_0$=425, p is the daily pressure value and p$_0$ = 606 g/cm^2 is the nominal pressure at the YBJ site. The two coefficient α and β are, respectively, the spectral index of the pad spectrum and the coefficient for the barometric effect. The normalized rate is showed by the red points in Fig.1.

The FWHM of the corrected rate distribution is about $\pm$ 2$\%$. However, we note some “runs” with rate much scattered from the average. A check of the detector conditions confirms that this effect is due to failures of the electronics as, for instance, a change of the threshold level of the RPC front-end, or a defect in the low voltage supplies of

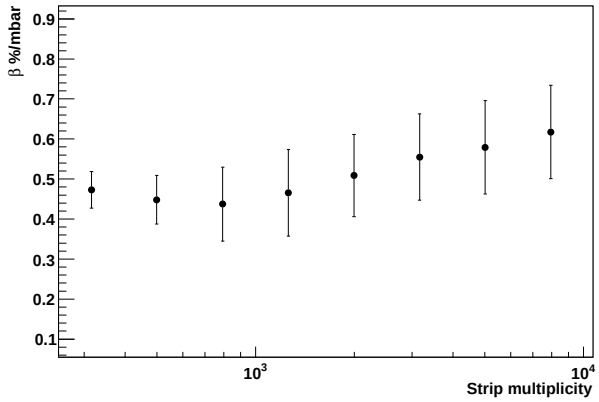

Figure 2: Barometric coefficient versus the strip multiplicity for events with zenith angle $\theta \leq 15^\circ$ and reconstructed core in A_{fid}.

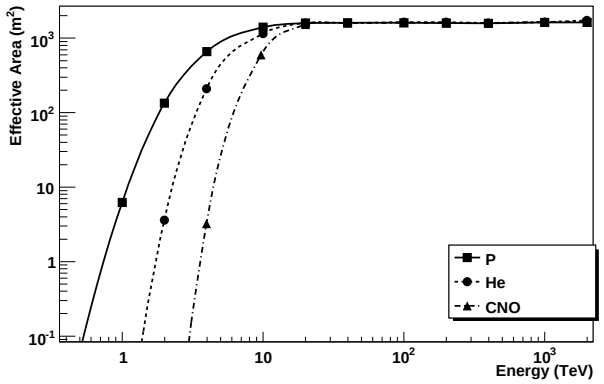

Figure 3: Effective areas for proton-, helium- and CNO-induced showers with $N_s > 400$ as a function of the primary energy.

the readout system. We excluded from the analysis all the data with a trigger rate outside the interval $\pm 3\%$ from the mean value. The gaps in the data stream correspond to maintenance periods. The selected events have been divided into "differential classes" defined by strip multiplicity ΔN_s. The width of the fired strip bins corresponds to $\Delta \mathrm{Log}(N_s) = 0.2$. For each bin, the measured rate has been corrected for the previous effects, for the dead time (4%) and for the average pad efficiency (95%). In Fig.2 the barometric coefficient β as a function of the shower multiplicity for quasi-vertical events ($\theta \leq 15^\circ$) is shown. The coefficient exhibits a dependence on the strip multiplicity.

4 Monte Carlo simulation

The air shower development in the atmosphere has been simulated with the CORSIKA v. 6.7.2 code [17]. The electromagnetic interactions are described by the EGS4 package while the hadronic interactions above 80 GeV are reproduced by the QGSJET-II.03 model. The low energy hadronic interactions are described by the FLUKA package. Cosmic rays have been generated in the energy range from 100 GeV to 4 PeV according to different spectra given in [2, 3]. About $\sim 10^9$ showers induced by protons, helium nuclei, CNO group and heavy nuclei have been sampled in the zenith angle interval 0° - 15°. The secondary particles have been propagated down to cut-off energies of 1 MeV (electromagnetic component) and 100 MeV (muons and hadrons). The experimental conditions (trigger logic, time resolution, electronic noises, relation between strip and pad multiplicities, etc.) have been taken into account via a GEANT3-based code. The core positions have been randomly sampled in an energy-dependent area large up to $3.5 \cdot 10^3 \times 3.5 \cdot 10^3$ m^2, centered on the detector. Simulated events have the same format used for the experimental data and are analyzed with the same reconstruction code.

The effective area $A_{eff}(E, >N_s)$, for events with core inside the fiducial area, is shown in Fig. 3 for showers with a strip multiplicity $N_s > 400$. These values are folded with the energy spectrum of each primary nucleus, to obtain the expected rate for each primary mass i

$$R_i(> N_s) = \int \Phi_i(E)\, A_{eff,i}(E, > N_s)\, dE\, d\Omega \qquad (2)$$

The expected integral rate of quasi vertical showers induced by protons, helium and CNO nuclei with CREAM spectra, reconstructed inside the fiducial area A_{fid}, is shown in Fig. 4.

The main contribution to the expected rate is provided by proton primaries. The contribution of the other nuclei increases with the strip multiplicity of the event. The relative fractions (in $\%$ of the total) $R_P/R_{He}/R_{CNO}/R_{heavy}$ are 67.6/28.2/2.7/0.7 in the first multiplicity bin (ΔN_S = 251-398) and 51.2/40.4/5.4/2.4 in the last multiplicity bin (ΔN_S = 6310 - 10000) for CREAM spectra. Proton- and helium-induced showers contribute to the rate for more than 90% in the whole strip multiplicity range. The CNO contribution is $< 7\%$, heavier nuclei contribute less than 3%.

5 Comparison with data

To obtain the light (p+He) component spectrum, we subtracted from the data the contribution of heavy elements, CNO, MgSi and Fe, calculated with the spectra shown in Fig. 4. In Fig. 5 the experimental event rate, without the contribution of heavy nuclei, is shown as a function of the strip multiplicity (stars) and compared to the expectations according to CREAM, Hörandel, JACEE and RUNJOB (p+He) spectra. The rate has been multiplied by $N^{1.25}$. The median energy for proton- (helium-) induced showers ranges from 4.5 (9) TeV (ΔN_S = 251-398) up to 56 (90) TeV (ΔN_S = 6310-10000). The statistical error on data is negligible, while the systematic uncertanty is estimated $\pm$ 10%, mainly due to the reconstruc-

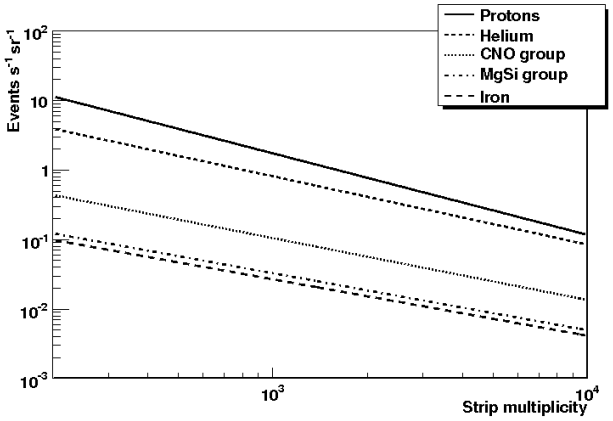

Figure 4: Expected integral rate of quasi vertical events with core in the fiducial area A_{fid} induced by protons, helium and CNO nuclei, calculated with spectra obtained by fitting the CREAM data.

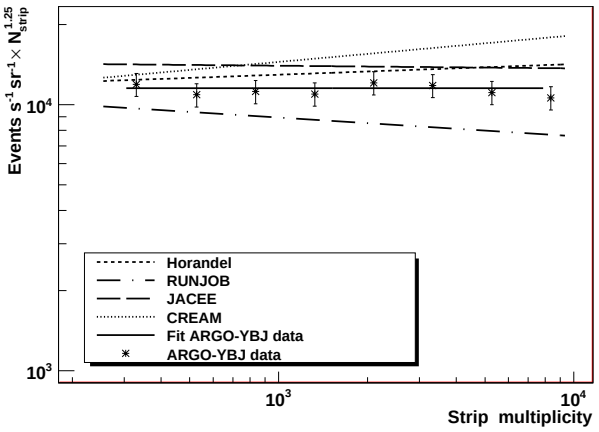

Figure 5: Comparison between the experimental data (stars) and the differential expected rates according to different spectra. The solid line is the best fit to data (see text for details).

tion of the core position. The different lines in Fig. 5 are best fits with the following spectral indices: -1.25±0.03 for data (solid line), -1.21±0.03 for H*ö*randel spectrum (short-dashed line), -1.32±0.03 for RUNJOB spectrum (dot-dashed line), -1.26±0.02 for JACEE spectrum (long-dashed line) and -1.15±0.03 for CREAM spectrum (dotted line). The uncertainties associated to different measurements are not shown in Fig. 5.

6 Conclusions

The high segmentation of the full coverage ARGO-YBJ detector and its location at high altitude allow the detection and the reconstruction of air showers induced by primary CRs of energies < 100 TeV. Selecting quasi-vertical showers with core located on a fiducial area inside the ARGO-YBJ central carpet, a sample of events mainly induced by proton and helium primaries is obtained.

The ARGO-YBJ data are consistent with JACEE and H*ö*randel expectations for what concern slope and flux and disfavour the RUNJOB helium measurement.

For the first time a ground-based measurement of the CR light component spectrum overlaps data obtained with direct methods for about two energy decades, providing a solid anchorage to the CR primary spectrum measurements in the knee region carried out by EAS arrays.

References

[1] H. S. Ahn et al., *ApJ Letters* 714, 2010, L89-L93.
[2] Y. S. Yoon et al., *ApJ* 728, 2011, 122-129.
[3] J.H. H*ö*randel, *Astrop. Phys.* 19, 2003, 193-220.
[4] K. Asakimori et al.,*ApJ* 502, 1998, 278-283.
[5] A.V. Apanasenko et al., *Astrop. Phys.* 16, 2001, 13-46.
[6] D. Caprioli et al., *Astrop. Phys.* 34, 2011, 447-456.
[7] M. Aglietta et al., *Astrop. Phys.* 21, 2004, 223-240.
[8] W.D. Apel et al., *Astrop. Phys.* 31, 2009, 86-91.
[9] M. Amenomori et al., *Phys. lett.* B632, 2006, 58-64.
[10] H. Tokuno et al., *Astrop. Phys.* 29, 2008, 453-460.
[11] Lagutin et al., Proc. of the *29th ICRC*, Pune **6** (2005) 77-80 (astro-ph/0507017).
[12] M. Aglietta et al., *Astrop. Phys.* 19, 2003, 329-338.
[13] G. Aielli et al., *NIM*, A562, 2006, 92-96.
[14] M. Iacovacci et al,, Proc. of the *31st ICRC* (2009).
[15] G. Di Sciascio et al., Proc. of the *28th ICRC*, Tsukuba (2003) 3015-3018.
[16] G. Di Sciascio et al., Proc. of the *29th ICRC*, Pune **6** (2005) 33-36.
[17] D.Heck et al.,*Report FZKA* 6019 (1998).